BEHAVIOR OF PARTIALLY DAMAGED CONCRETE-FILLED DOUBLE SKIN TUBULAR STUB COLUMNS UNDER FIRE

AMIN HEIDARPOUR[1] and XIAO-LING ZHAO[2]

[1]*Department of Civil Engineering, Monash University, Melbourne, VIC 3800, Australia*
E-mail: amin.heidarpour@monash.edu
[2]*School of Civil and Environmental Engineering, The University of New South Wales, Sydney, NSW 2052, Australia*
E-mail: xiaolin.zhao@unsw.edu.au

The concrete-filled double skin tubular (CFDST) sections are known as a type of steel-concrete composite members consisting of outer and inner steel skins while the gap between steel skins is filled by concrete. This composite member has gained popularity in infrastructure construction, e.g. piers and columns, due to several advantages including but not limited to high load carrying capacity, high energy absorption due to deformation of inner steel tube, high local stability due to interaction between steel and concrete, and great performance under fire. It has been identified, however, that there exists a limited research regarding the behavior of CFDST columns under 'accident' conditions involving the combined effects of initial damage followed by fire exposure. Therefore, this paper addresses a series of experimental tests conducted on circular CFDST stub columns fabricated from Self-Compacting Concrete (SCC) and Grade 350 structural mild steel. Specimens are subjected to four discrete tests; quasi-static compression to failure at ambient temperature, and low-, medium- and high-damage tests caused by quasi-static loading at room temperature followed by fire in a gas furnace. The results of experiments give an insight into the relationship between varying level of prior partial damage and the respective reduction in member capacity under fire conditions.

Keywords: Concrete-filled double skin, partial damage, stub columns, fire, self-compacting concrete.

1 Introduction

The concrete-filled double skin tubular (CFDST) section is a type of steel-concrete composite member, widely used for piers and columns (Zhao and Han, 2006). CFDST elements consist of an outer and inner steel skin confining self-compacting concrete (SCC) (Lu, 2010). CFDST sections are a further revision of the composite concrete-filled tubular (CFT) section. The hollow steel core maintains high section stiffness while reducing member self-weight. It has been found that the external skin behaves similarly to that of a CFT section, however the internal skin behaves similar to an unfilled hollow section (Zhao and Han, 2006). This composite design has gained popularity in infrastructure construction due to several advantages such as increased load carrying capacity (Zhao, et al. 2010); increased energy absorption due to deformation of inner steel tube; decreased noise and vibration due to self-compacting nature of concrete; high local stability due to interaction between steel and concrete, and preventing concrete from spalling by steel skins (Kodur, 1998).

Proceedings of the 17th International Symposium on Tubular Structures.
Editors: X.D. Qian and Y.S. Choo

Published by Research Publishing, Singapore.
ISBN: 978-981-11-0745-0; doi:10.3850/978-981-11-0745-0_047-cd

CFDST sections have been the subject of extended research aimed to identify the behavior of such members under various failure conditions. Currently, comprehensive research has investigated the behavior of CFDST sections under fire loading, high-lighting the benefits of composite design under fire exposure (Lu, 2010). Additionally, prior research has addressed the high deformation capacity of CFDST elements (Zhao, et al. 2010). It has been identified however, that there exists an absence of research regarding the behavior of CFDST columns under 'accident' conditions involving the combined effects of initial damage caused by quasi-static loading followed by fire exposure. Given the potential hazard to life arising from the failure of structural columns, this knowledge is deemed critical for safe structural design. This paper reconciles this knowledge gap through a series of tests on CFDST stub columns. The key objective of this research is to gain an understanding of the effects of varying levels of prior axial damage on the fire endurance of CFDST stub columns under quasi-static loading. The experimental program will only assess stub columns in order to isolate the failure mechanisms and eliminate premature global buckling of members.

2 Material Properties

The CFDST specimens are comprised of two materials; Grade 350 steel tubes (CHS) and self-compacting concrete (SCC). Compressive tests of the cold-formed CHS specimens determined a yield stress of 357MPa. SCC is a critical component of CFDST design due to its high workability (Lu, 2010) and ease of construction without the need for concrete compaction. The use of SCC has been found to more effectively maintain the interaction between steel and concrete, thus improving composite action (Zhao and Han, 2006). The SCC mix design used for this research is outlined in Table 1.

Table 1. SCC design mix

Component	Quantity (kg/m^3)
Water	180
Cement	122
Fly ash	153
Slag	153
Fine aggregate	865
Coarse aggregate	817
Superplasticiser	2.3 (L)

The design mix included a high proportion of fine aggregate in order to limit segregation. The coarse aggregate was crushed basalt ranging from 10 to 15mm in size, as this allowed for sufficient flow through the annulus between the two steel skins. Given the importance of workability, slump tests were conducted to ensure adequate flow. Standard concrete cylinders were prepared to determine the compressive strength of the SCC. The average compressive strength ($f'_{c.50\ days}$) and slumps are 48.1 MPa and 525mm, respectively.

3 Stub Column Specimens

CFDST stub columns were fabricated using circular hollow sections (CHS) for both the inner and outer skins. Each steel specimen was measured for thickness, diameter/width and length at numerous locations. The test specimen geometry is summarized in Table 2. In total, four concrete-filled CHS specimens were fabricated.

Table 2. CFDST specimen geometry

Specimen	d_{outer} **(mm)**	t_{outer} **(mm)**	d_{inner} **(mm)**	t_{inner} **(mm)**	L **(mm)**	A_c **(mm^2)**
CC1	218.75	4.9	100.50	3.0	500.0	26345
CC2	218.75	4.9	100.75	3.1	500.0	26322
CC3	218.75	4.9	101.00	3.1	500.0	26298
CC4	219.00	5.0	100.75	3.0	500.0	26361

4 Experimental Programme

4.1 *Quasi-static Compression Test at Ambient Temperature*

The CC1 sample was subjected to a quasi-static compression test under ambient temperature conditions. The test was undertaken using the Amsler compression machine available at Civil Engineering Department, Monash University as shown in Figure 1.

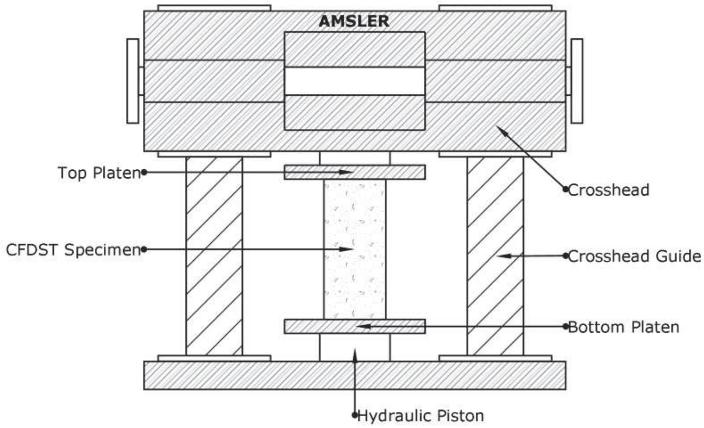

Figure 1. Compression test setup under Amsler machine

The load, platen position and strains were recorded using a data acquisition system. Specimens were fitted with 6 strain gauges; 4 spaced at 90° along the centreline and 2 spaced 100mm from each end of the sample. This setup is shown in Figure 2.

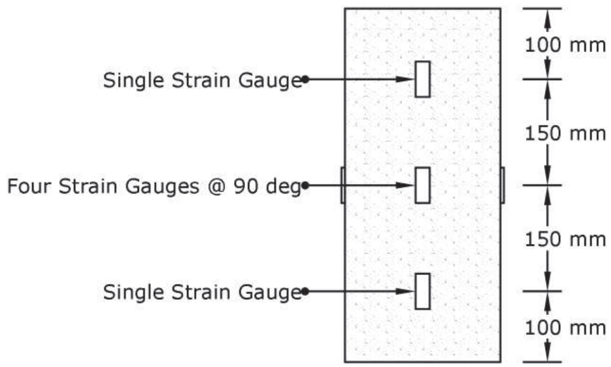

Figure 2. Strain gauge setup

During compression, the platens were restricted in all but axial translation creating a double fixed-end condition. This ensured that the potential of premature buckling was not exacerbated by platen rotation. The compression test was conducted on CC1 at a displacement rate of 2mm/min until ultimate capacity was reached and a moderate drop in load was observed. The resultant force-strain curve was used in the determination of discrete levels of damage. Thus, similar quasi-static compression test was done on the CFDST samples (CC2-CC4) up to discrete strain points determined from the force-strain relationship developed for the CC1. The partially-damaged CC2-CC4 specimens were then subject to fire test as explained in the next section.

4.2 *Quasi-static Compression Test under Fire*

The partially damaged specimens were subjected to a standard fire test in a furnace in which the temperature rose following the ISO834 curve. Before starting the fire test, a quasi-static compression load equivalent to approximately 70% of the ultimate capacity was applied to the specimens. This aimed to give a representation of the 'at-service' loading. Given the deformation of the sample, the load would fluctuate; therefore the pressure of the hydraulic piston was manually adjusted to maintain the desired force (±2%). The fire test setup is shown in Figure 3.

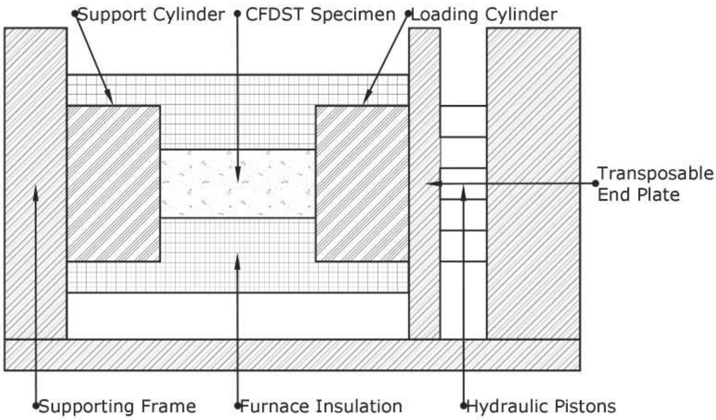

Figure 3. Fire test setup

The temperature was recorded using Type K thermocouples. The thermocouples were attached at discrete locations to give an accurate representation of the heat propagation through and around the sample. The thermocouples were attached to both the inner and outer tubes according to the layout shown in Figure 4. The vertical line of three thermocouples was aligned with the fire source and the bottom thermocouple offset by 90 degrees was aligned with the furnace exhaust. During the experiment the temperature rose according to the standard fire test function until the sample was unable to support the quasi-static compression load any further. According to AS1530.4 (2005), the criteria for structural adequacy failure of the specimen include the following conditions:

- Deformation exceeds 1% of member length; and
- Rate of deformation exceeds 0.3% of member length per minute.

It was found that the rate of deflection criterion was always met before the deflection criterion, therefore only the deformation failure was measured.

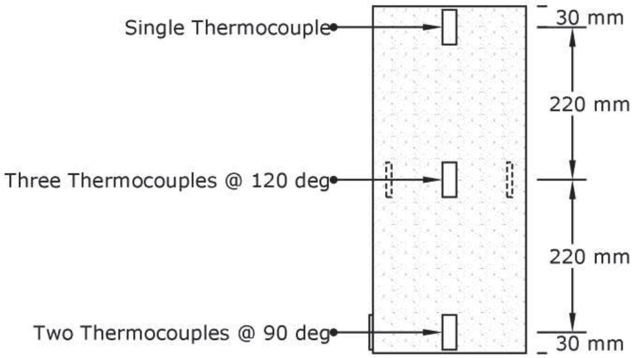

Figure 4. Thermocouple setup

5 Experimental Results

5.1 *Ambient Quasi-static Compression Test*

The static compression test on CC1 produced the force-strain curve shown in Figure 5. The experiment produced a yield force of 2460kN corresponding to a yield strain of 0.36%. The ultimate capacity of the sample was determined to be 2711kN. This force-strain curve was then used to determine three discrete damage levels including low damage (LL = 0.40%), medium damage (MD = 1.20%), and high damage (HD = 2.0%) levels corresponding to CC2, CC3 and CC4 specimens, respectively. It is noted that due to the variability of compressive strength between the samples, the load corresponding to each damage level for each specimen varied from the reference sample by up to 5.0%.

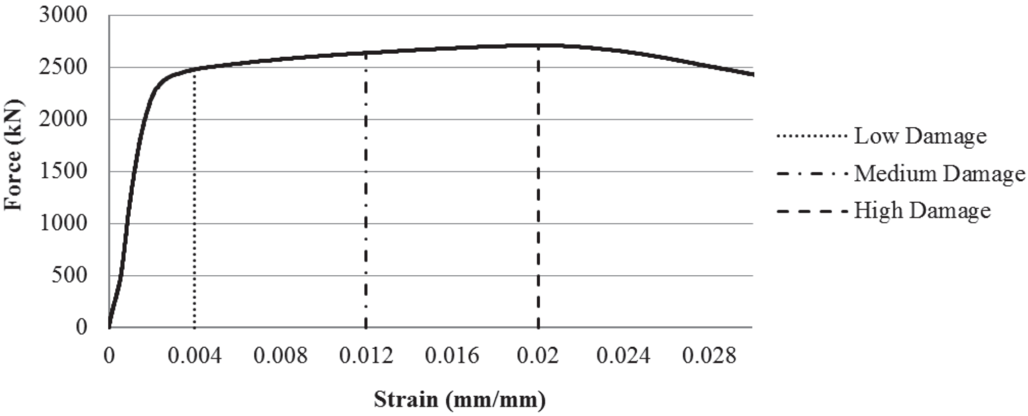

Figure 5. CC1 force-strain curve under ambient temperature

5.2 *Fire Tests Results*

As explained above, each partially-damaged specimen was tested in the furnace under a quasi-static compression load. Given the ultimate capacity determined in the previous section, the 70% quasi-static applied load was 1900kN. The critical temperatures and duration of heating for each sample are summarized in Table 3. The displacement-time curves for each damaged specimen are also shown in Figure 6. The experiments undertaken give a clear insight into the effect of damage on the fire endurance of partially damaged

CFDST specimens. The specimens which were exposed to greater levels of damage and inherently greater strain levels, exhibited reduced fire endurance under a static axial load.

Table 3. Sample failure time and temperature

	Low Damage (CC2)	Medium Damage (CC3)	High Damage (CC4)
Time (min)	94.3	85.0	78.8
Furnace Temperature (°C)	1013.0	997.4	986.0
Critical Temperature (Outer) (°C)	877.0	843.6	834.8
Critical Temperature (Inner) (°C)	590.9	570.0	534.2

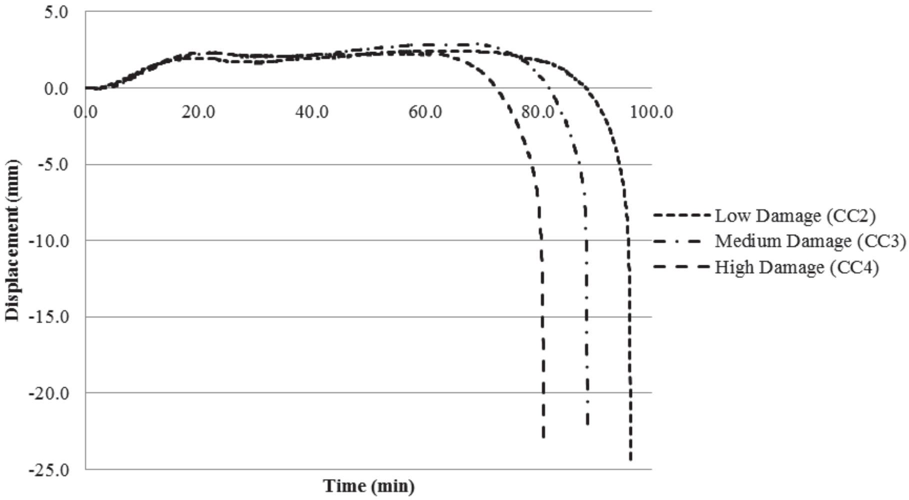

Figure 6. Displacement-time curve for low damage, medium damage and high damage specimens

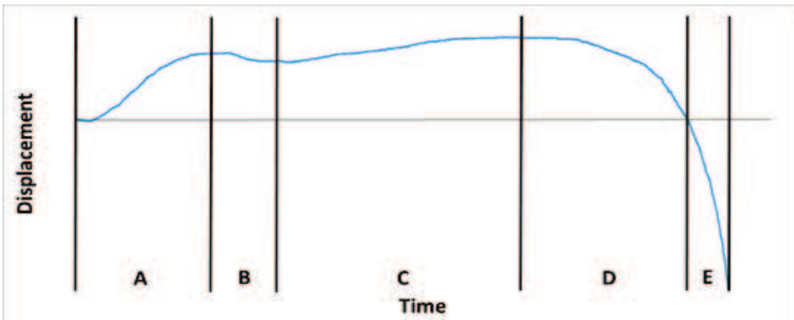

Figure 7. Typical displacement-time curve for partially damaged specimens under fire

The fire tests identified several key stages in the axial deformation of the specimens when subjected to fire loading. Figure 7 shows a typical displacement-time curve. In Stage A, the sample experienced positive deformation corresponding to the expansion of the outer steel skin under increasing temperature. The outer skin capacity began to reduce as the temperature increased resulting in the contraction observed in Stage B. As the temperature propagated through the sample, the inner skin began to expand. This effect can be observed in Stage C, where the specimen once again experiences positive deformation. The inner skin capacity began to reduce as the temperature increased resulting in the contraction observed in Stage D. The contraction is much more rapid than in Stage B given that the sample is significantly weakened by this point. Lastly, in Stage E, both steel skins have undergone expansion and contraction and the specimen is generally close to failure. This stage can be identified by a large and exponentially increasing rate of deformation. The double-expansion observed is a result of the heating of the two concentric steel tubes and poses a unique benefit; the staggered expansion creates two points of resistance, the expansion of outer skin followed by the inner skin. In later stages of fire loading, the expansion of the internal tube may potentially extend the fire endurance of the specimen by reducing the load taken by the more critically heated component (external skin). This effect can be generally observed by CFDST sections experiencing a longer period of expansion than CFT sections.

Figure 8 shows the temperature-time curve for CC2. Note that the temperature-time curves for CC3 and CC4 exhibited similar trend to that of CC2 and have not been shown here. From Figure 8, it is understood that the specimens were positioned such that the fire source aligned with the central thermocouples and the exhaust with the bottom thermocouples. The temperature propagation along the outer skin was therefore expected; the specimen center experienced the highest temperature and the bottom experienced the lowest. The outer skin temperature followed a logarithmic curve, similar to the logarithmic function of the furnace. Due to the insulation of the concrete, the heat propagation to the internal skin was delayed and demonstrated almost linear growth.

The failure mechanisms of CC1 and CC4 samples have been shown in Figure 9. The partially-damaged stub columns subject to fire loading experienced a failure mechanism similar to CC1 with less localized deformation. The failure of all fire samples demonstrated similar characteristics; i.e. medium sized bulge adjacent to the cross-head on external skin, and wide central bulge on external skin and small central bulge on internal skin.

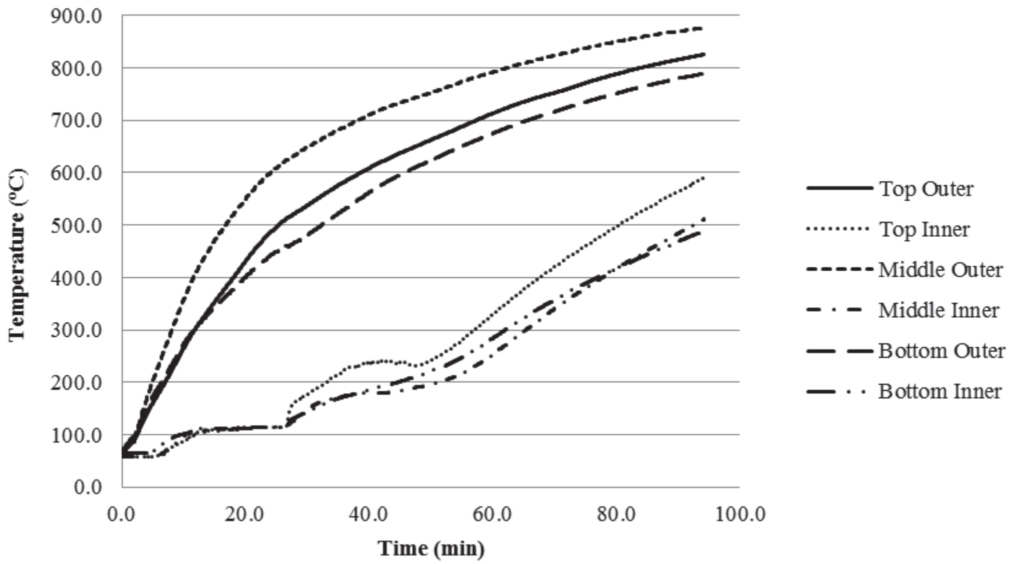

Figure 8. Temperature-time curve under fire for CC2 specimen

CC1: AS @ 0º CC1: AS @ 90º CC1: AS @ 180º CC1: AS @ 270º

CC4: HD @ 0º CC4: HD @ 90º CC4: HD @ 180º CC4: HD @ 270º

Figure 9. Failure mechanism of CC1 at ambient state (AS) and CC4 specimens

6 Conclusion

This paper presented the experimental study regarding the effects of prior damage on the fire endurance of concrete-filled double skin tubular stub columns. CFDST specimens were subjected to axial damage corresponding to strains of 0.4%, 1.2% and 2.0%. The stub columns were then loaded with 1900kN representing approximately 70% of ultimate capacity, and subjected to a standard fire test. It was observed that an increase in strain deformation (higher damage levels) produced a reduction in the fire endurance under a static axial load. An increase of strain damage from 0.4% to 2.0% resulted in a reduction of fire endurance from 877.0ºC (94.3mins) to 834.8ºC (78.8mins).

Acknowledgement

This work presented in this paper was supported by the Australian Research Council through the Discovery Project DP150100442. The authors thank Mr Anton Shilo for his help in conducting the experiments, and also laboratory staff of Civil Engineering Department at Monash University.

References

AS 1530.4: Methods for fire tests on building materials, components and structures – Fire resistance test of elements of construction, Sydney, Australia, 2005.

Kodur, V.K.R., Performance of high strength concrete-filled steel columns exposed to fire. *Canadian Journal of Civil Engineering*, 25(6): p. 975-981, 1998.

Lu, H., Fire Behaviour of Self-Consolidating Concrete-Filled Double Skin Steel Tubular Columns, PhD thesis, Monash University, Melbourne, Australia, 2010.

Zhao, X.L. and Han, L.H. *Double skin composite construction. Progress in Structural Engineering and Materials*, 8(3): 93-102, 2006.

Zhao, X.L., Tong, L.W., and Wang, X.Y. CFDST stub columns subjected to large deformation axial loading. *Engineering Structures*, 32(3): 692-703, 2010.